J. Mater. Environ. Sci. 6 (12) (2015) 3483-3490 *Aatiq et al.*
ISSN : 2028-2508
CODEN: JMESCN

Structure and spectroscopic characterization of the two $PbSb_{0.5}Fe_{1.5}(PO_4)_3$ and $Pb_{0.5}SbFe(PO_4)_3$ phosphates with Nasicon type-structure

A. Aatiq*, My R. Tigha, R. Fakhreddine, A. Marchoud

Université HassanII de Casablanca, Faculté des Sciences Ben M'Sik, Département de Chimie, Laboratoire de Physico-Chimie des Matériaux Appliqués, Avenue Idriss El harti, B.P. 7955, Casablanca, Morocco.

**Corresponding Author e-mail: a_aatiq@yahoo.fr ; Tel: (+212670816543)*

Abstract

Two newly synthesised $Pb_{0.50}SbFe(PO_4)_3$ [$Pb_{0.5}$] and $PbSb_{0.50}Fe_{1.50}(PO_4)_3$ [Pb] phases were obtained by conventional solid state reaction techniques at 900°C in air atmosphere. Their crystallographic structures were determined at room temperature from X-ray powder diffraction (XRPD) data using the Rietveld analysis. Both compounds belong to the Nasicon structural family. [$Pb_{0.5}$] and [Pb] crystallise in rhombohedral system with R $\bar{3}$ and R $\bar{3}$c space group respectively. Hexagonal cell parameters for [$Pb_{0.5}$] and [Pb] are: a = 8.2397(1) Å, c = 22.7801(2)Å, and a = 8.313(1) Å, c = 23.000(2) Å, respectively. Pb^{2+} and vacancies in $\{[Pb_{0.50}]_{3a}[\square_{0.50}]_{3b}\}_{M1}SbFe(PO_4)_3$ are practically ordered within the two positions, 3a and 3b, of M1 sites. Structure refinements show also an ordered distribution of Sb^{5+} and Fe^{3+} ions within the Nasicon framework. Within the structure, each $Pb_{(3a)}O_6$ octahedron shares two faces with two $Fe^{3+}O_6$ octahedra and each vacancy ($\square_{(3b)}O_6$) site is located between two $Sb^{5+}O_6$ octahedra. In $[Pb]_{M1}Sb_{0.50}Fe_{1.50}(PO_4)_3$ compound, all M1 sites are occupied by Pb^{2+} and the Sb^{5+} and Fe^{3+} ions are randomly distributed within the Nasicon framework. A Raman and Infrared spectroscopic study was used to obtain further structural information about the nature of bonding in both selected compositions.

Abbreviations: $Pb_{0.50}SbFe(PO_4)_3$ = [$Pb_{0.5}$], $PbSb_{0.50}Fe_{1.50}(PO_4)_3$ = [Pb]

Keywords: Lead, Antimony and Iron phosphate, Nasicon structure, Raman and IR spectroscopy, Rietveld analysis.

Introduction

The Nasicon-type family has been the subject of intensive research due to its potential applications as solid electrolyte, electrode material, and low thermal expansion ceramics and as storage materials for nuclear waste [1-7]. The structure of such materials with general formula $A_xXX'(PO_4)_3$ consists of a three-dimensional network made up of corner-sharing $X(X')O_6$ octahedra and PO_4 tetrahedra in such a way that each octahedron is surrounded by six tetrahedra and each tetrahedron is connected to four octahedral. Within the Nasicon framework, there are interconnected interstitial sites usually labelled M1 (one per formula unit) and M2 (three per formula unit) through which A cation can diffuse, giving rise to a fast-ion conductivity [1,3,7] (Fig.1). The four such sites per formula unit can be represented by the crystallographic $[M2]_3[M1]XX'(PO_4)_3$ formula. Each M1 cavity is situated between two $X(X')O_6$ octahedra along the c-axis. Six M2 cavities with eightfold coordination are located between the $[O_3X(X')O_3M1O_3X(X')O_3\square O_3X(X')O_3]_\infty$ ribbons and surround the M1 cavity (Fig.1).

Recently, the structural characteristics by powder X-ray diffraction (XRPD) study using the Rietveld method for $A_{0.50}SbFe(PO_4)_3$ (A = Mn, Ca, Cd, Sr) (R $\bar{3}$ space group) and $ASb_{0.50}Fe_{1.50}(PO_4)_3$ (A = Ca, Sr) (R $\bar{3}$c space group) Nasicon phases were realised [8-11]. In all $A_{0.50}SbFe(PO_4)_3$ samples, A^{2+} cations occupied principally one-half of the M1 3a sites and the Sb^{5+} and Fe^{3+} cations are orderly distributed within the $SbFe(PO_4)_3$ framework. In a continuation of our search concerning Nasicon-like structure, in this paper, we report the results of the structural investigations by the Rietveld refinement using the X-ray powder diffraction patterns (XRPD), of $Pb_{0.50}SbFe(PO_4)_3$ and $PbSb_{0.50}Fe_{1.50}(PO_4)_3$ compositions. In order to obtain further structural

information about the nature of bonding in the crystalline solids, a Raman and Infrared spectroscopic study was also undertaken.

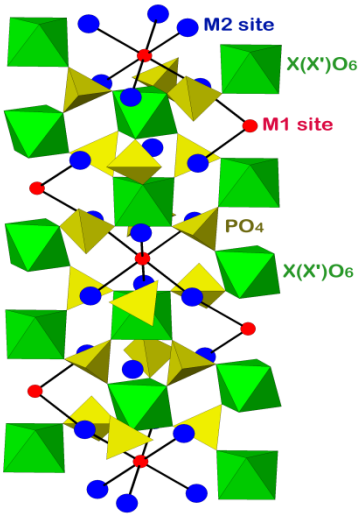

Figure 1: Crystal structure, along c-axis, of the rhombohedral $[M2]_3[M1]XX'(PO_4)_3$ Nasicon-type.

2. Materials and methods

Syntheses of $Pb_{0.50}SbFe(PO_4)_3$ and $PbSb_{0.50}Fe_{1.50}(PO_4)_3$ phases were carried out using conventional solid-state reaction techniques. Powder crystalline samples were prepared from mixtures of carbonates $Pb(NO_3)_2$ (Riedel-de Haën, 99 %), oxides Sb_2O_3 (Riedel-de Haën, 99.9 %), Fe_2O_3 (Prolabo, 99 %) and $NH_4H_2PO_4$ (Riedel-de Haën, 99 %) in stoichiometric proportions. The mixture was heated progressively with intermittent grinding at 200°C (12h), 400°C (6h), 600°C (12h), 800°C (24h) and 900°C (24h) in air atmosphere. The products of reaction were characterised by X-ray diffraction (XRD) at room temperature with a Panalytical X′Pert-PRO (θ-2θ) diffractometer; (CuKα) radiation (45 kV, 40 mA); divergence slit of 1° and antiscatter slit of 1°. The data were collected from 10 to 90° 2θ, in steps of 0.008°, with a counting time of 30 s per step. The Rietveld refinement of the structure was performed using the Fullprof program [12].

The infrared spectra are recorded in the form of KBr pellets in the wave number range 1500-400 cm^{-1} using a Bruker's VERTEX 70 spectrometer and the Raman spectra are recorded on RENISHAW 1000B spectrometer in the wave number range 100–1500 cm^{-1}. All the spectra have been recorded at room temperature.

3. Results and discussion

Analysis of the XRPD spectra of [Pb] and [$Pb_{0.5}$] indicated that the peak positions of the XRPD lines are similar to those observed for other Nasicon-type phases (Fig. 2 and Fig. 3). $PbSb_{0.50}Fe_{1.50}(PO_4)_3$ is isostructural with $SrSb_{0.50}Fe_{1.50}(PO_4)_3$ ($R\bar{3}c$ space group) Nasicon-type phase [10]. The presence, in XRPD pattern of $Pb_{0.50}SbFe(PO_4)_3$, of diffraction peaks with Miller indexes h0l (l = 2n+1) (e.g., (101) and (003) reflections) is incompatible with the plane c. Therefore, the XRPD data of [$Pb_{0.5}$] are consistent with R32 and $R\bar{3}$ space groups. The structural refinements of [Pb] and [$Pb_{0.5}$], were principally based upon the previous assumption.

3.1. Structure of $PbSb_{0.50}Fe_{1.50}(PO_4)_3$

The structural parameters of $SrSb_{0.50}Fe_{1.50}(PO_4)_3$ [10] were used as starting parameters for the Rietveld refinement of $PbSb_{0.50}Fe_{1.50}(PO_4)_3$. Refinement with all Pb atoms in the M1 site and Sb(Fe) within the Nasicon framework leads to best results (R_B = 3.6%). The final reliability factors and atomic parameters for [Pb] are summarised in Table 1. A comparison of the experimental and calculated XRPD profile is shown in Figure 2. Pb-O(2) (2.640(2) Å) and Sb(Fe)-O (Sb(Fe)-O(1) = 1.910(3) Å, Sb(Fe)-O(2) = 1.987(3) Å) distances values are consistent with the ionic radii values in six coordination of Pb^{2+}, Sb^{5+} and Fe^{3+}ions [13]. P-O distances values, 1.525(3) Å and 1.512(2) Å, match well with those typically observed in Nasicon-type phosphates. XRPD data of, obtained from the ‘‘observed intensities’’ of the Rietveld refinement (CuKα1: 1.540 56 Å), are presented in Table 2. Note that diffraction lines with I_{obs}< 1 are omitted.

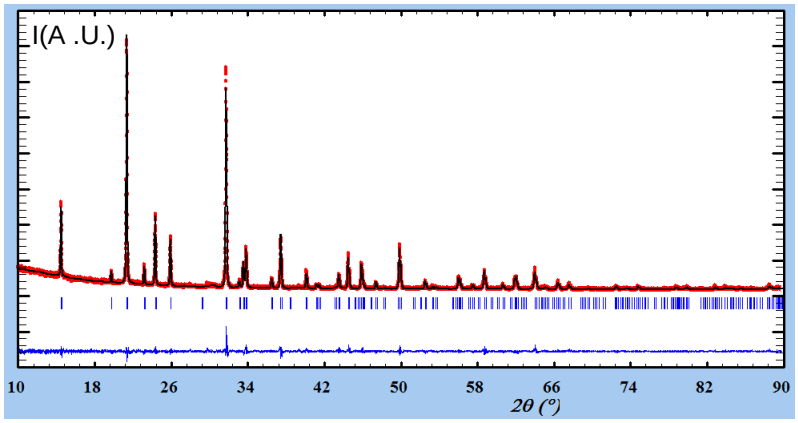

Figure 2: Experimental (•••) calculated (—), and difference profile (—) of the XRD pattern of $PbSb_{0.50}Fe_{1.50}(PO_4)_3$.

Table 1: Results of the Rietveld refinement of $PbSb_{0.50}Fe_{1.50}(PO_4)_3$.

$PbSb_{0.50}Fe_{1.50}(PO_4)_3$						
Space group, $R\bar{3}c$; [Z = 6; $a_{hex.}$ = 8.313(1) Å; $c_{hex.}$ = 23.000(2) Å; V = 1377(1) $Å^3$]						
Profile parameters						
Pseudo-voigt function, PV = ηL + (1-η)G; η = 0.204(5)						
Half-width parameters, U = 0.077(4), V = -0.037(3), and W = 0.014(2)						
Conventional Rietveld R-factors, R_{WP} = 6.7%; R_P = 5.1%; R_B = 3.6%; R_F = 3.1%						
Atom	site	Wyckoff positions			$B_{iso}(Å^2)$	Occupancy
Pb	6b	0	0	0	2.4(1)	1
Sb(Fe)	12c	0	0	0.1507(2)	0.4(1)	0.50(1.50)
P	18e	0.2846(3)	0	0.25	0.3(1)	1
O(1)	36f	0.1628(5)	-0.0502(5)	0.1959(3)	1.4(1)	1
O(2)	36f	0.4732(5)	0.1682(4)	0.2389(3)	1.4(1)	1

Table 2: Powder diffraction data of $PbFe_{1.5}Sb_{0.5}(PO_4)_3$ ($CuK\alpha_1$; λ = 1.540 56 Å).

hkl	**d_{obs} (Å)**	**100 *I/I₀* (obs.)**	**100 *I/I₀* (cal.)**	***hkl***	**d_{obs} (Å)**	**100 *I/I₀* (obs.)**	**100 *I/I₀* (cal.)**
012	6.1025	31	28	1 1 12	1.7406	3	3
104	4.4930	5	5	404	1.7178	2	1
110	4.1569	100	100	137	1.7065	1	1
006	3.8333	8	7	318	1.6401	5	5
113	3.6543	30	31	232	1.6350	4	4
202	3.4356	20	19	0 1 14	1.6017	2	2
116	2.8180	90	81	410	1.5711	8	7
211	2.7025	3	3	048	1.5256	2	2
018	2.6700	10	10	0 3 12	1.4977	5	5
122	2.6482	16	15	2 0 14	1.4946	5	5
214	2.4597	5	4	146	1.4538	8	7
300	2.4000	20	21	238	1.4322	1	1
208	2.2465	7	6	1 2 14	1.4064	4	3
1 0 10	2.1909	2	2	330	1.3856	2	2
119	2.1771	2	2	425	1.3048	1	1
220	2.0784	6	6	336	1.3031	1	2
036	2.0342	14	13	3 1 14	1.2687	2	1
128	1.9764	10	10	1 4 12	1.2151	1	1
312	1.9675	3	3	600	1.2000	2	1
0 0 12	1.9167	3	3				
226	1.8271	18	17				

3.2. Structure of $Pb_{0.50}SbFe(PO_4)_3$

Structure determination of $Pb_{0.50}SbFe(PO_4)_3$, using the Rietveld method, was undertaken in two principle models. In the first model the refinement was made in R32 space group whereas in the second the hypothesis of $R\bar{3}$ space group was verified. During the first model, initial starting parameters for the Reitveld Refinements of $[Pb_{0.5}]$, using R32 space group, were based on those already reported for $Na_5Ti(PO_4)_3$ ($[Na_3]_{M2}[Na]_{M1}TiNa(PO_4)_3$ crystallographic formula) [14]. Pb^{2+} and vacancies are randomly distributed in the M1 site, 6c position (0 0 ~0.25), while Sb^{5+} and Fe^{3+} are supposed to reside within the framework. The refine ment in this model was confirmed to be less appropriate. During the second model, the structural parameters of $[Sr_{0.50}\square_{0.50}]_{M1}SbFe(PO_4)_3$ in $R\bar{3}$ space group [10] were used as starting parameters for the Rietveld refinement. In a first step, Pb^{2+} ions are supposed to reside only in one of the two possible types of M1 site, 3a (000); the other, 3b (001/2), was considered to be empty. Sb and Fe atoms were constrained to be distributed, within the framework, between the two possible types of 6c position. Note that in the final step of refinement, the Pb atoms were allowed to occupy the two possible positions of M1 sites (3a and 3b) instead of only 3a in the previously refinement. In this refinement only 0.08(1) of Pb^{2+} ions are found in 3b position of M1 site. This last result agrees well with an ordered cationic distribution of Pb^{2+} within the M1 sites. Since the experimental XRD pattern of $Pb_{0.50}SbFe(PO_4)_3$ also has diffraction peaks from a small amount (about 8 wt.%) of the $PbSb_{0.50}Fe_{1.50}(PO_4)_3$, the Rietveld refinement was carried out using a two phase model, consisting of $Pb_{0.50}SbFe(PO_4)_3$ and the $PbSb_{0.50}Fe_{1.50}(PO_4)_3$ which crystallizes with the $R\bar{3}c$ space group. This last refinement leads to acceptable reliability factors. Observed, calculated, and difference XRD patterns are given in Figure 3. The final reliability factors and atomic parameters for $[Pb_{0.5}]$ are summarised in Table 3.

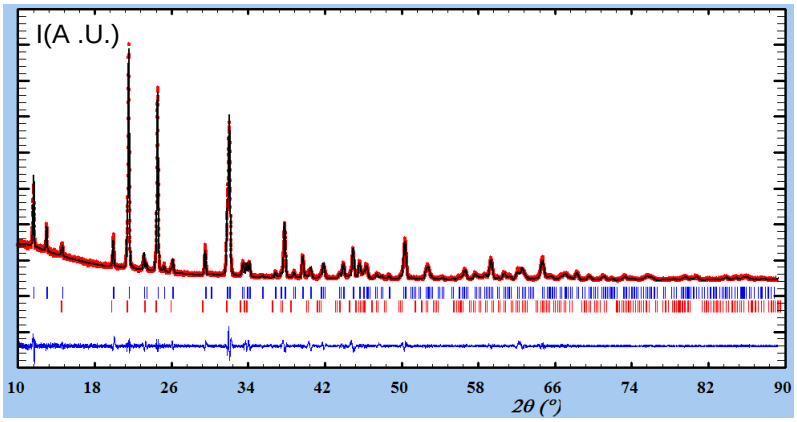

Figure 3: Experimental (•••) calculated (—), and difference profile (—) of the XRD pattern of $Pb_{0.50}SbFe(PO_4)_3$. The positions of the Bragg reflections (top $Pb_{0.50}SbFe(PO_4)_3$, bottom $PbSb_{0.50}Fe_{1.50}(PO_4)_3$) are shown by small vertical lines.

Table 3: Results of the Rietveld refinement of $Pb_{0.50}SbFe(PO_4)_3$.

$Pb_{0.50}SbFe(PO_4)_3$						
Space group, $R\bar{3}$; [Z = 6, a = 8.2397(3) Å, c = 22.7801(8) Å; V = 1339(1) Å^3]						
Profile parameters						
Pseudo-voigt function, PV = ηL + (1-η)G; η= 0.205(2)						
Half-width parameters, U = 0.1923(2), V= -0.090(1), and W = 0.056(2)						
Conventional Rietveld R-factors, R_{WP} = 7.6 %; R_P = 6.3 %; R_B = 4.1%; R_F = 3.0 %						
Atom	site	Wyckoff positions			B_{iso}(Å^2)	Occupancy
Pb(1)	3a	0	0	0	2.4(2)	0.92(1)
Pb(2)	3b	0	0	0.5	2.4(2)	0.08(1)
Fe(Sb)(1)	6c	0	0	0.1483(4)	0.6(1)	0.94(0.06)(1)
Sb(Fe)(2)	6c	0	0	0.3492(4)	0.4(1)	0.94(0.06)(1)
P	18f	0.2932(5)	0.0030(6)	0.2481(2)	0.6(1)	1
O(1)	18f	0.4924(5)	0.1615(4)	0.2369(3)	1.2(2)	1
O(2)	18f	0.2778(6)	-0.1856(6)	0.2631(2)	1.2(2)	1
O(3)	18f	0.1722(5)	-0.0434(6)	0.1933(3)	1.2(2)	1
O(4)	18f	0.2047(4)	0.0759(5)	0.2919(4)	1.2(2)	1

Their structure is represented in Figure 4. In order to facilitate the structure description, we use in the following $Pb_{(3a)}O_6$ to define the site occupied to 92 % by Pb^{2+} and $\square_{(3b)}O_6$ for the site which contains 8 % of Pb^{2+} ions. The presence of a quasi-ordered vacancy-strontium distribution leads to two inequivalent FeO_6 and SbO_6 octahedra. Each $Pb_{(3a)}O_6$ octahedron shares two faces with two FeO_6 octahedra and each weakly occupied ($\square_{(3b)}O_6$) site is located between two SbO_6 octahedra. Note that refinement of the occupancy rate of Sb and Fe atoms within the two possible crystallographic 6c positions leads to a value of 0.06 for Sb in (0 0 ~0.35) 6c position and 0.06 for Fe in (0 0 ~0.14) 6c position (Table 3). The electrostatic repulsion between the two O(2) triplets surrounding the vacant 3b M1 sites tends to increase its volume. In fact, the $\square_{(3b)}$-O(2) = 2.659(2) Å distance is superior to that of the $Pb_{(3a)}$-O(1) one (2.618(3) Å) (Figure 4). The Fe-O interatomic distances (Fe-O(1) = 1.853(3) Å ; Fe-O(3) = 1.923(3) Å) show that the FeO_6 octahedra, which have a common face with the occupied $Pb_{(3a)}O_6$ octahedra are relatively more distorted than the SbO_6 octahedra (Sb-O(2) = 1.945(3) Å ; Sb-O(4) = 1.971(3) Å) which share one face with the unoccupied $\square_{(3b)}O_6$ octahedra. This result can be related to the electrostatic repulsion between Pb^{2+} and the neighbouring Fe^{2+} ions within the $[..O_3FeO_3Pb_{M1(3a)}O_3FeO_3\square O_3SbO_3\square_{M1(3b)}O_3SbO_3..]_\infty$ ribbons (Figure 4). Since the ionic radii values of Sb^{5+} and Fe^{3+} cations are relatively comparable, the exact reason behind the tendency of a quasi-ordering of the Sb^{5+} and Fe^{3+} cations, within $Pb_{0.50}SbFe(PO_4)_3$ Nasicon framework, may be related to the difference between their oxidation state. Indeed, in order to minimise the electrostatic repulsion between neighbouring cation within the ribbons, two $Fe^{3+}O_6$ octahedra tend to juxtapose the quasi-full occupied M1(3a) sites. In contrast, the unoccupied M1(3b) sites have practically two $Sb^{5+}O_6$ octahedra as a neighbouring. The P-O distance values (P-O(1) = 1.523(3) Å ; P-O(2) = 1.533(3) Å ; P-O(3) =1.523(3) Å ; P-O(4) =1.525(3) Å) are in good agreement with those typically observed in Nasicon-like phosphates. XRPD data of [$Pb_{0.5}$], obtained from the ‘‘observed intensities’’ of the Rietveld refinement (CuKα1: 1.540 56 Å), are presented in Table 4**.**

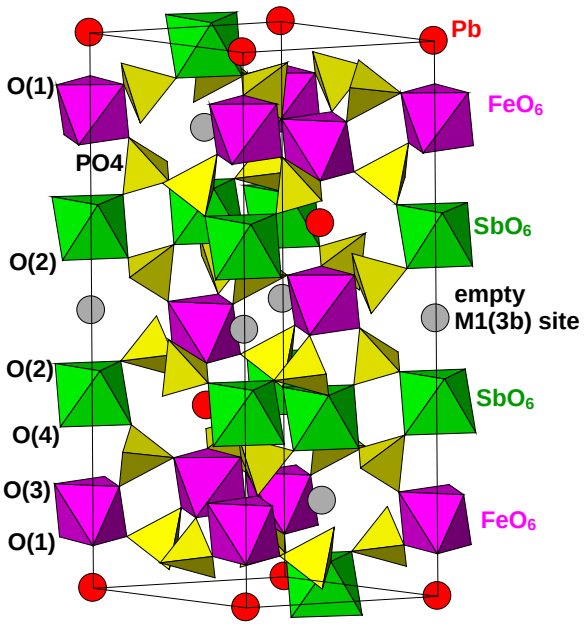

Figure 4: Perspective view, along c-axis, of the structure of $Pb_{0.50}SbFe(PO_4)_3$.

3.3. Raman and Infrared spectroscopy

In order to obtain further structural information about the nature of bonding in both [Pb] and [$Pb_{0.5}$] crystalline solids, in this part of the paper, a Raman and Infrared (IR) spectroscopy study was undertaken. The IR and Raman spectra of [Pb] and [$Pb_{0.5}$] are shown in Figures 5a and 5b respectively. Spectra of both samples are similar except the broad Raman band observed for [Pb]. According to the crystallographic results, the relatively broadening Raman bands observed in [Pb] spectra (Fig. 5b), in comparison to those found in the [$Pb_{0.5}$] Raman ones, may be easily related to the difference between the cationic distributions within both Nasicon frameworks. In fact, both Pb^{2+} ions in M1 sites and Sb^{5+}(Fe^{3+}) within the $Pb_{0.5}SbFe(PO_4)_3$ Nasicon framework are relatively orderly distributed. Consequently, in this last material, every PO_4 group is surrounded by two FeO_6 octahedra and two SbO_6 octahedra. In the case of $PbSb_{0.5}Fe_{1.5}(PO_4)_3$, the stoichiometric consideration

(75% of Fe and 25% of Sb atoms within the framework) leads to several combinations for the PO_4 group environments. So, in [Pb.] sample, the PO_4 groups are more disturbed and consequently in addition to the broadening of the Raman bands, shifts of the modes to higher or lower wavenumbers (red or blue shift) are normally expected.

Table 4: Powder diffraction data of $Pb_{0.5}FeSb(PO_4)_3$ ($CuK\alpha_1$; λ = 1.540 56 Å).

hkl	d_{obs} (Å)	100 I/I_0 (obs)	100 I/I_0 (cal)	*hkl*	d_{obs} (Å)	100 I/I_0 (obs)	100 I/I_0 (cal)
003	7.5933	26	30	0 2 10	1.9200	3	2
101	6.8095	13	13	0 0 12	1.8983	1	1
012	6.0470	4	3	134	1.8694	2	2
104	4.4512	13	8	315	1.8152	8	8
110	4.1198	100	100	226	1.8106	19	16
015	3.8400	7	7	2 1 10	1.7403	4	4
006	3.7967	2	2	309	1.7333	7	7
113	3.6212	85	82	1 1 12	1.7241	2	2
021	3.5249	4	3	137	1.6909	1	1
202	3.4047	5	5	1 2 11	1.6425	1	1
024	3.0235	15	12	318	1.6251	4	4
205	2.8090	32	32	229	1.5977	3	3
116	2.7919	72	77	0 1 14	1.5864	2	2
211	2.6783	7	4	140	1.5571	10	7
018	2.6447	5	7	413	1.5254	3	3
122	2.6245	7	4	048	1.5117	2	1
214	2.4375	3	2	1 3 10	1.4902	4	4
300	2.3786	25	21	3 0 12	1.4837	5	4
125	2.3209	3	2	2 0 14	1.4805	4	5
033	2.2698	10	8	146	1.4407	10	9
208	2.2256	4	4	4 0 10	1.4045	2	2
119	2.1566	6	6	1 0 16	1.3962	3	2
217	2.0766	2	2	1 2 14	1.3932	3	3
220	2.0599	7	6	330	1.3733	3	3
036	2.0157	13	10	0 4 11	1.3516	2	2
223	1.9880	4	4	419	1.3262	2	1
128	1.9581	7	7	336	1.2914	2	2
312	1.9499	3	3				

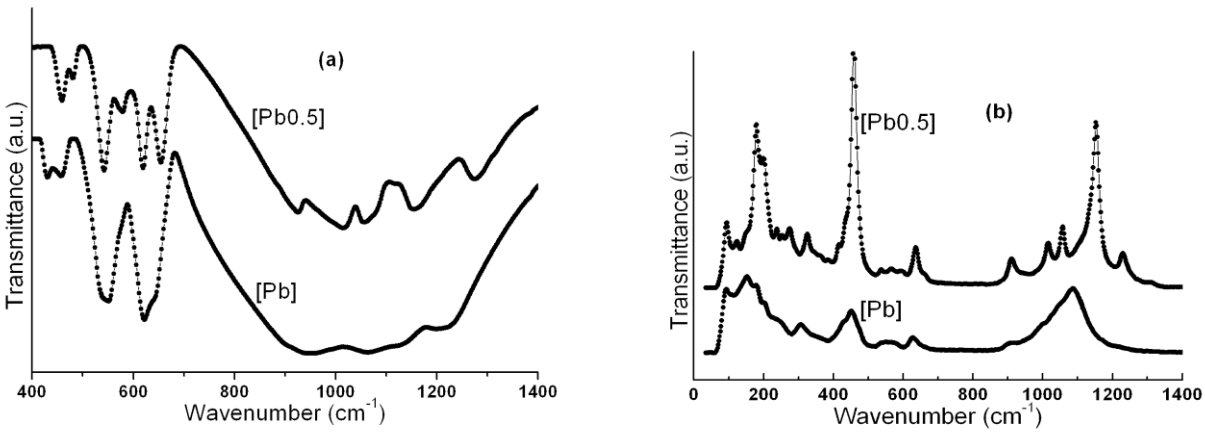

Figure 5: IR (a) and Raman (b) spectra of $Pb_{0.5}SbFe(PO_4)_3$ ([$Pb_{0.5}$]) and $PbSb_{0.5}Fe_{1.5}(PO_4)_3$ ([Pb]).

The vibration modes of Nasicon phases can be assigned to internal and external modes of (PO_4) tetrahedra and to lattice modes including the motions of the metallic Sb^{5+} and Fe^{3+} in their octahedral coordination and Pb^{2+} ions in six coordination spheres. It is observed that phosphate group vibrations are generally strong compared to

the lattice modes and metal-oxygen vibrations. According to factor group analysis, the phosphate PO_4 tetrahedra group has Td symmetry and nine internal modes ($\Gamma_d = A_1 + E + 2F_2$).
The Raman and IR band positions of the four (ν_1, ν_2, ν_3 and ν_4) modes observed in the spectra of [Pb] and [$Pb_{0.5}$] Nasicon phases are close to those expected for Nasicon type materials. Assignments of Infrared and Raman vibration modes of [Pb] and [$Pb_{0.5}$] are gathered in Table 5. Thus, the symmetric non degenerate PO stretching modes (ν_1) are observed in the range 900-1063 cm^{-1} while antisymmetric doubly degenerate PO stretching (ν_2) are located in the 410-480 cm^{-1} range. The symmetric, triply degenerate OPO bending (ν_3) is observed between 1090-1150 cm^{-1} and the triply degenerate, antisymmetric and harmonic OPO bending (ν_4) is observed in the range 540-650 cm^{-1}. Note that all the modes are Raman active except the ν_3 and ν_4 ones which are IR active only.

Table 5: Assignments of Infrared and Raman vibration modes of $Pb_{0.5}SbFe(PO_4)_3$ and $PbSb_{0.5}Fe_{1.5}(PO_4)_3$.

$PbSb_{0.5}Fe_{1.5}(PO_4)_3$		$PbSb_{0.50}Fe_{1.50}(PO_4)_3$		Assignments
Raman	IR	Raman	IR	
	1275	1230		$\nu(PO_4)$ / ν(MO)
			1200	interaction
	1154	1154	1150	$\nu_3(PO_4)$
1090				
1050	1056	1060	1063	$\nu_1(PO_4)$
1000	1015	1016		
900	925	911	950	
630	650	636	622	ν_s(SbO)
580	620	600		
550	580	560	550	$\nu_4(PO_4)$
540	545	540		
470	481	470	460	$\nu_2(PO_4)$
451	458			
430		430	430	
		410		
330		325		ν_s (Fe^{3+}-O)
305				
		274		External modes
		250		
240		240		
200		200		
175		180		
154		150		
		124		
94		95		

The SbO_6 octahedra are distorted and exhibit a low symmetry. The Sb-O…P bonds existing in [Pb] and [$Pb_{0.5}$] compounds have an average length of 2.00 Å. Their stretching vibrations are probably coupled with the P-O-P bending ν_4 mode. The frequencies found between 580 and 650 cm^{-1} in Raman and IR spectra can be assigned empirically to Sb-O stretching modes involving Sb-O-P linkage. The same Sb–O vibrations are already observed, in the IR spectrum of $SbOPO_4$ at 597 and 652 cm^{-1} [15] and at 580 and 639 cm^{-1}, in the IR and Raman spectra, of $Mn_{0.5}MSb(PO_4)_3$ (M = Al, Fe and Cr) phases [16]. Obtained results are also in good agreement with the spectroscopic study realised for $Sr_{0.50}SbFe(PO_4)_3$ and $NaSbFe(PO_4)_3$ [10,17]. Note that in the both samples the IR and Raman data confirm the presence of Sb^{5+} in octahedral oxygen coordination. In the lattice modes region, the translational modes of Pb^{2+}, Fe^{3+}, Sb^{5+} and PO_4^{3-} ions as well as librational modes of PO_4^{3-} ions and FeO_6 and/or SbO_6 groups should be expected. At wavenumbers below 450 cm^{-1} strong coupling between the different bending vibrations O-P-O, O-Sb-O, Sb-O-P, Sb-O-Sb is expected [18].
The Raman bands observed at 330 and 305 cm^{-1} in [Pb] and [$Pb_{0.5}$] (Figure 5b), could be assigned to Fe^{3+}-O stretching modes of vibrations. It can be seen that similar band positions are observed in the range 300-370 cm^{-1} of the $Li_3Fe_2(PO_4)_3$ Raman spectrum [19] and also at 375 and 308 cm^{-1} for $NaSbFe(PO_4)_3$ phase [17]. The low frequency modes observed below 275 cm^{-1} can be easily attributed to translational modes of the Pb^{2+}, Sb^{5+} and $(PO_4)^{3-}$ ions.

Conclusion

$Pb_{0.50}SbFe(PO_4)_3$ and $PbSb_{0.50}Fe_{1.50}(PO_4)_3$ compounds are prepared and characterized by XRPD, Raman and IR spectroscopy. Both the samples crystallise in hexagonal lattice of the Nasicon framework with the space group $R\bar{3}$ for [$Pb_{0.5}$] and $R\bar{3}c$ for [Pb]. The Rietveld analysis results of the refinement show that Sb^{5+} and Fe^{3+} ions are randomly distributed within the [Pb] framework whereas the same cations are orderly distributed within the [$Pb_{0.5}$] framework one. This last ordering cationic distribution may be related to the difference between the Sb^{5+} and Fe^{3+} oxidation state.
Raman and IR spectra are consistent with [$Pb_{0.5}$] and [Pb] crystal structures. The spectra show characteristic PO_4 vibrations. The stretching modes of SbO_6 groups are observed at significantly higher frequency (580 and 650 cm^{-1}) than stretching modes of FeO_6 groups (~330 cm^{-1}).

Acknowledgements
The authors are grateful to Engineers (in Service Centrale d'Analyse (CSA) de l'Unités d'Appui Technique à la Recherche Scientifique (UATRS)" CNRS- Rabat, Morocco) for technical assistance; and for Centre CSA of CNRS- Rabat (Morocco) for making to the disposal of our Laboratory a Panalytical X'Pert-PRO diffractometer.

References

1. Hong H.Y.P., *Mat. Res. Bull.* 11 (1976) 173.
2. Roy R., Vance E. R., Alamo J., *Mat. Res. Bull.* 17 (1982) 585.
3. Delmas C., Viala J. C., Olazcuaga R., Le Flem G., Hagenmuller P., Cherkaoui F., Brochu R., *Solid State Ionics* 3/4 (1981) 209.
4. Woodcock D. A., Lightfoot P., Smith R. I., *J. Mater. Chem.* 9 (1999) 2631.
5. Aatiq A., Ménétrier M., El Jazouli A., Delmas C., *Solid State Ionics* 150 (2002) 391.
6. Padhi A. K., Nanjundaswamy K. S., Masquelier C., Goodenoogh J. B., *J. Electrochem. Soc.* 144(8) (1997) 2581.
7. Aatiq A., Ménétrier M., Croguennec L., Suard E., Delmas C., *J. Mater. Chem.* 12 (2002) 2971.
8. Aatiq A., Hassine R., Tigha MyR., Saadoune I., *Powder Diffr.* 20 (2005) 33.
9. Aatiq A., Tigha MyR., Hassine R., Saadoune I., *Powder Diffr.* 21 (2006) 45.
10. Aatiq A., Tigha MyR., Benmokhtar S.**,** *J. Mater. Science* 47 (2012) 1354.
11 Aatiq A., Tigha MyR., Attaoui A., Nadi N. and El Bouari A., *MATEC Web of Conferences* 5 (2013) 4018.
12. Rodriguez-Carvajal J., *Physica B* 192 (1993) 55.
13. Shannon R. D., *Acta Crystallogr Sect, A Cryst. Phys. Diffr. Theor. Gen. Crystallogr.* 32 (1976) 751.
14. Krimi S., Mansouri I., El Jazouli A., Chaminade J .P., Gravereau P., Le Flem G., *J. Solid State Chem.* 105 (1993) 561.
15. Sudarsan, V., Muthe K.P., Vyas J.C., Kulshreshtha S.K., *J. Alloys Compd.* 336 (2002) 119.
16. Anantharamulu N., Rao K. K. , Vithal M., Prasad G., *J. Alloys Compd*. 479 (2009) 684.
17. Aatiq A., Tigha R., *Powder Diffr.* 28/S2 (2013) S394.
18. Husson E., Genet F., Lachgar, A., Piffard, Y., *J. Solid State Chem.* 75 (1988) 305.
19. Butt G.**,** Sammes N.**,** Tompsett G.**,** Smirnova A., Yamamoto O., *J. Power sources* 134 (2004) 72.
20. Rao K. J., Sobha K. C., Sundeepkumar A., *Proc. Indian Acad. Sci*. 113 (2001) 497.